

Investigation of Transmission Raman Scattering Light Collection and Raman Spectrum Analysis

Satoshi Makita, Michihiko Ikeda

[Summary]

Precision sensing is a key technology for building a safe and stable society, and attention is focused on Raman spectroscopy as one optical measurement technology supporting non-contact and non-destructive sensing. Consequently, we investigated high-sensitivity measurement of Raman scattering and Raman spectrum analysis methods. This article considers optical-fiber coupling efficiency and transmission Raman scattering intensity in transmission Raman spectrometers with extremely low Raman scattering light collection efficiency used for analyzing the internal components of materials. Additionally, it introduces an analysis method using Raman spectrum analysis with an example of assaying aqueous ethanol solutions using basic Classical Least Squares (CLS) and Multiple Linear Regression (MLR) multi-variate analyses.

1 Introduction

With industrial development and diversifying lifestyles, precision sensing technology is becoming increasingly important for accurate capture, analysis, and support of reliable data to build a secure and safe society.

Among available sensing technologies, non-contact and non-destructive optical measurement technologies cover a very wide application range including: optical-fiber sensor technology for monitoring dark fiber and building structural applications; precision measurement technology using laser interference, refraction, polarization, scattering, etc.; optical-evaluation technology using light to evaluate various materials; bioinstrumentation technology including microscopy and optical interference tomography; ultra-short-optical-pulse measurement technology; light sources and optical measurement devices, etc.

The key points for optical measurement technologies are designing optical systems for accurate capture of physical phenomena including the wavelength, phase, amplitude, polarization, non-linearity of the optical wave as well as finding the optimum balance in the tradeoff between measurement precision and speed.

Recent advances in semiconductor technology have resulted in development of high-performance laser light sources and detectors used in various optical measurement equipment, and there is increasing interest in Raman spectroscopy offering both high spectrum resolution and free-space resolution to expand the application market.

This article introduces some tests of high-sensitivity

sensing systems using Raman spectroscopy as well as Raman spectrum analysis methods.

2 Raman Spectroscopy

2.1 What is Raman Scattering?

When a material is irradiated by light, phenomena such as reflection, transmission, absorption, scattering occur, depending on the interaction between the light and the material. At scattering, the light path changes irregularly according to the material particles. When investigating the spectrum of the scattered light from a material irradiated by monochromatic light, rather than observing light with the same length as the incident light (Rayleigh scattering), we observe light with different wavelengths from the incident light, which is Raman scattering. As shown in Figure 1, Raman scattering appears only at a wavelength shifted by the molecular vibration energy corresponding to the incident light (excitation light). The amount of the excitation-light wavelength shift is called the Raman shift and is expressed as wave numbers that are a reciprocal of the wavelength. There are two types of Raman scattering: 1. Stokes Raman scattering shifted to the long wavelength side, and 2. Anti-Stokes Raman scattering shifted to the short wavelength side. In Raman spectroscopy, generally, the higher-level Stokes Raman scattering is observed. However, even Stokes Raman scattering is extremely weak with a level of only 10^{-6} compared to Rayleigh scattering.

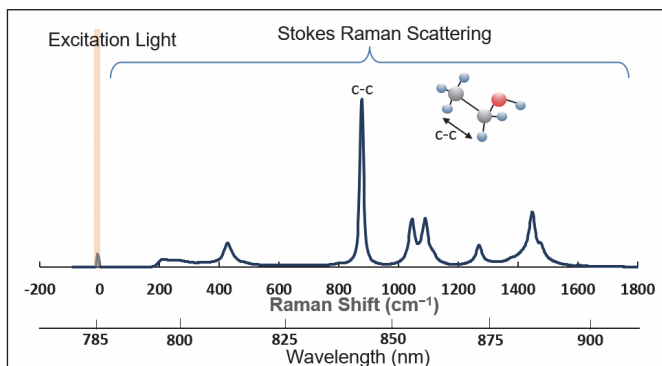


Figure 1 Raman Spectrum of Ethanol

2.2 What is Learned from Raman Scattering?

Raman scattering includes various information related to the molecular structure and it is possible to analyze the detailed molecular structure from the Raman spectrum. For example, Figure 1 shows the Raman spectrum for ethanol ($\text{C}_2\text{H}_5\text{OH}$) as an example with a large Raman shift peak close to 850 cm^{-1} due to the C-C bond vibration. As shown, since the Raman spectrum indicates a unique value determined by the material molecular structure, it can be used for material identification, quantification, and component analysis. Additionally, as shown in Figure 2, the shape of the Raman spectrum can be used for analyzing the concentration of the material, the crystallinity degree of crystalline materials, and the various molecular states, including distortion of the crystal lattice.

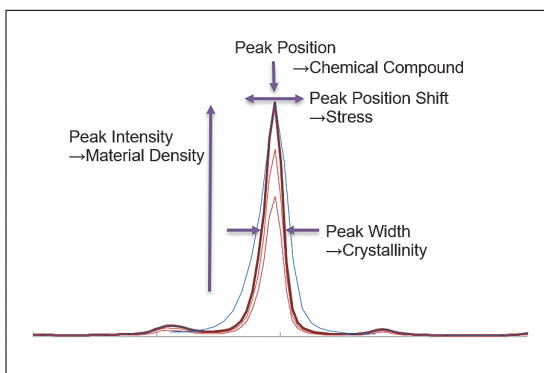


Figure 2 What is Learned from Raman Spectrum

2.3 Raman Spectroscope

Figure 3 shows two examples of Raman spectroscope configurations. Figure 3(a) is an example of a spot analysis system for measuring Raman scattering at a very small area on the surface of the test material. Figure 3(b) shows an example of transmission Raman analysis for measuring Raman scattering inside a test material. The excitation light emitted by the light source passes via the optical irradiation system to irradiate the material and the scattered light resulting

from the excitation light irradiation is output to the spectroscope after passing via the optical collecting system. Since this scattered light includes the extremely intense Rayleigh scattering, a notch filter is used to remove the excitation light so that only Raman scattering is output to the spectroscope. The Raman scattering light is converted to an electrical signal by the spectroscope detector and this electrical signal is processed to capture the Raman spectrum.

The main parts of the Raman spectrometer are explained below.

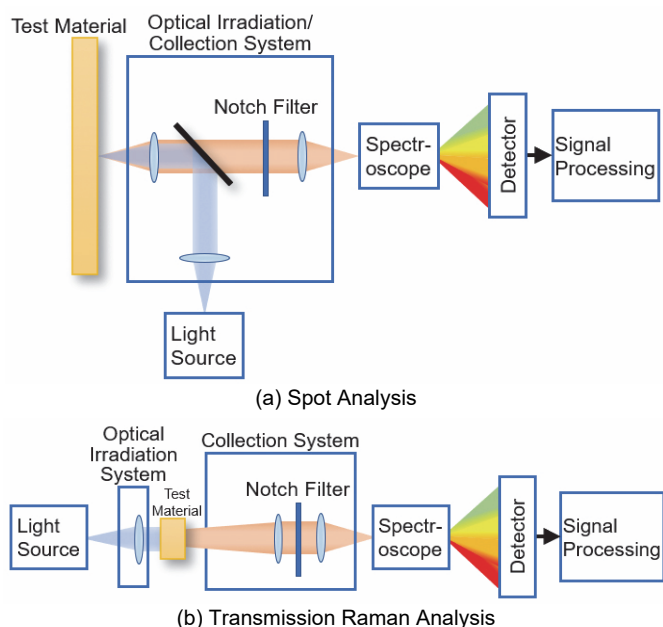


Figure 3 Example of Raman Spectroscopic Configuration

(1) Light Source

An excitation light source with high spectral purity is required to obtain the necessary resolution at the Raman spectrometer. In addition, a high-output laser light source is required because the Raman scattering intensity is proportional to the power of the excitation light source.

Since the Raman scattering intensity is proportional to the fourth power of the excitation light angular oscillation frequency, intense Raman scattering is obtained as the excitation light wavelength gets shorter. However, when measuring fluorescent materials that interfere with Raman spectroscopy, it is better to use a longer-wavelength light source causing less fluorescence. Additionally, in consideration of detector sensitivity and general costs, it is better to use light sources with wavelengths of 405, 488, 532, or 785 nm. More recently, near-infrared laser light sources with a wavelength of 1064 nm are being used to suppress the impact of fluorescence.

(2) Optical Irradiation and Light Collection System

The arrangement of the excitation light irradiation optical system and the Raman scattering light collection systems differ according to the material to be measured and the measurement method. Moreover, the Raman spectroscope design for the optical irradiation and collection systems is important because the Raman scattering light is extremely weak, so the excitation light must irradiate the test material efficiently and the Raman scattering light generated by this irradiation must be collected efficiently too.

Generally, the Raman spectroscope excitation light irradiates a spot on the material surface as shown in Figure 3(a) and the optical system is designed as a backscatter optical system to guide the generated Raman scattering to the spectroscope. Using spot analysis, Raman spectroscopy supports very small materials of just a few microns in size to analyze the components at the surface of the test material. The excitation light irradiation and Raman scattering light collection optical systems are integrated into one system.

More recently, the focus has been on transmission Raman analysis systems for analyzing the internal components of materials. As shown in Figure 3(b), the transmission Raman spectroscope uses separate excitation light irradiation and Raman scattering light collection systems. The Raman scattering light is attenuated and widened by transmission through the test material. As a result, the light-collection efficiency of the transmission Raman spectroscope is much lower than the spot analysis system, making measurement more difficult. The details are explained in the next section.

(3) Spectroscope

Figure 4 shows the basic structure of the spectroscope. The output beams from the optical fiber pass via the entrance slit and are made parallel via the collimator mirror. The parallel beams from this mirror are divided by the diffraction grating before reflection by the camera mirror to form an image at the CCD sensor. Since the entrance-slit image is reformed at the pixels of the detector CCD, the width of the input slit is proportional to the wavelength resolution. Improving the wavelength resolution requires narrowing the entrance slit, but since this reduces the amount of light, there is a trade-off relationship between the dynamic range and wavelength resolution.

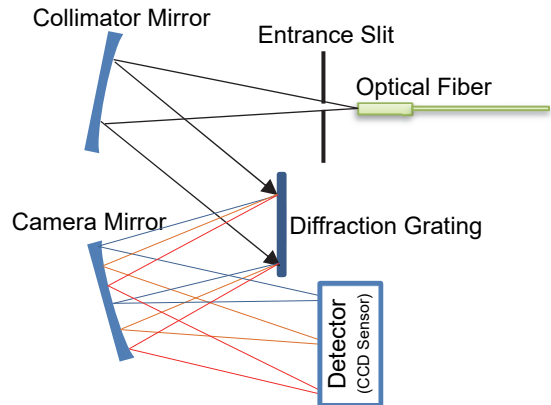


Figure 4 Basic Structure of Spectroscope

(4) Detector

Most Raman spectrometers use a CCD sensor with many parallel silicon (Si) light-reception elements for good sensitivity to visible light. Since the CCD sensor must be able to measure multiple wavelengths all at once, short measurement time is an advantage. On the other hand, an InGaAs (indium gallium arsenide) sensor with sensitivity to the near-infrared is used when using excitation light with a wavelength of 1064 nm to suppress the effect of fluorescence.

3 Transmission Raman Scattering Light Collection

This section describes Raman scattering light collection in the transmission Raman spectrometer for analysis of material internal components. In the transmission Raman spectrometer, Raman scattering light collection efficiency is extremely low because the light is attenuated and widened several mm by passage through the test material. Consequently, testing collection of transmission Raman scattering light is important.

3.1 Optical Fiber Coupling Efficiency

As shown in Figure 5, to inject light efficiently into optical fiber the light incident angle θ_{in} must not exceed the maximum incident angle $\theta_{in\ max}$, which is determined by the optical fiber NA (Numerical Aperture). For a step-index multimode optical fiber with a fixed core and cladding index of refraction (IoR), the NA is determined by the core IoR n_{core} and cladding IoR n_{clad} as expressed in Eq. (1)

$$NA = n \sin \theta_{in\ max} = \sqrt{n_{core}^2 - n_{clad}^2} \quad (1)$$

where, n is the IoR of the optical fiber external medium. For example, in air ($n = 1$), from Eq. (1), $\theta_{in\ max}$ is 12.7° for fiber with an NA of 0.22. In other words, light exceeding an incident angle of 12.7° leaks outside a fiber with an NA of 0.22 NA and cannot propagate along the core. To inject light

efficiently into the optical fiber, it is best to use a fiber with a large NA and large core diameter. However, even using this type of fiber, as described in section 2.3(3), the spectroscope entrance slit imposes limits on the amount of light passing to the detector.

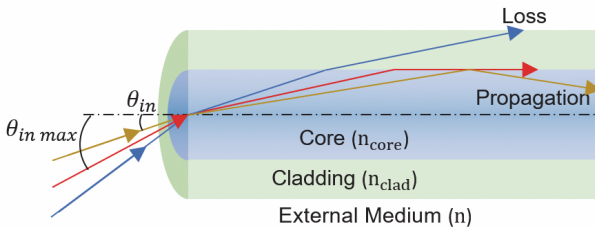


Figure 5 Optical Fiber NA

3.2 Spot Raman Scattering Coupling Efficiency

Raman scattering light generated when illuminating one spot of the test material with excitation light is thought of as being radiated isotropically. At this time, the coupling efficiency η of the Raman scattering incident to the fiber is found from the ratio of the solid angle in the range of the optical-fiber incident angle θ_{in} to the solid angle in the entire sphere as shown in Eq (2)

$$\eta = \frac{2\pi L^2(1-\cos\theta_{in})}{4\pi L^2} \quad (2)$$

$$L \leq \frac{r}{NA} \quad \theta_{in} = \theta_{in max}$$

$$L > \frac{r}{NA} \quad \theta_{in} = \tan^{-1} \frac{r}{L}$$

where, L is the distance between the excitation-light irradiation spot and the optical-fiber end face, and r is the optical-fiber core diameter. As shown in Figure 6, when L is small, the possible coupling angle θ_{in} to the optical fiber is the maximum incident angle determined by the optical fiber NA. When L is large, the coupling efficiency drops because only part of the Raman scattering widen at maximum incident angle enters the optical-fiber core. Accordingly, the most efficient Raman scattering incident angle is achieved when $L \leq \frac{r}{NA}$.

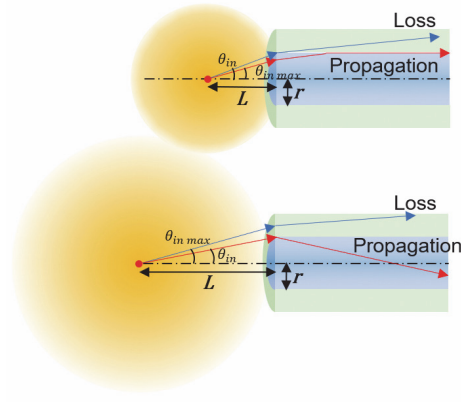


Figure 6 Spot Raman Scattering Coupling Efficiency

3.3 Transmission Raman Scattering Coupling Efficiency

This section considers the coupling efficiency when widen Raman scattering light after passage through the test material is incident to the optical fiber. As shown in Figure 7(a), Raman scattering light from point P can be incident to the fiber at incident angle θ_{in1} to θ_{in2} . The coupling efficiency is found in the same way as described in the previous section as the ratio of the solid angle in the range of the optical-fiber incident angle to the solid angle in the entire sphere. If the distance L between the test material surface and the fiber end face is constant, when the distance x between the point P and the optical-fiber center axis becomes bigger than x_{max} shown in Eq. (3), the coupling efficiency drops as θ_{in2} becomes bigger than the optical fiber maximum incident angle $\theta_{in max}$ in Figure 7(b).

$$x_{max} = L \cdot \tan \theta_{in max} - r \quad (3)$$

To receive scattering light of radius R , L from Eq. (3) must satisfy Eq. (4).

$$L = \frac{R+r}{\tan \theta_{in max}} \quad (4)$$

At this time, the coupling efficiency of the point-P scattering light from $R \ll L$ approaches Eq. (2) at $\theta_{in} = \tan^{-1} \frac{r}{L}$.

If the power of the excitation light is the same, it is thought that the total amount of generated Raman scattering light is equal independent of the irradiated area; the Raman scattering light coupling efficiency is determined by the optical fiber incident angle. Accordingly, L must become bigger as R increases as the test-material surface transmission Raman scattering becomes wider, so the optical-fiber coupling efficiency drops. For example, when injecting transmission Raman scattering for $R=5$ mm into an optical fiber with a core diameter of 200 μ m and an NA of 0.22, $L=22.6$ mm and the coupling efficiency is about 34 dB lower than for spot Raman scattering.

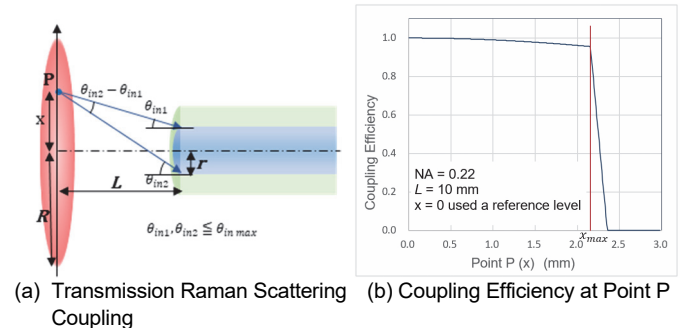


Figure 7 Transmission Raman Scattering Coupling

3.4 Opaque-Material Raman Scattering Intensity

This section considers the test-material attenuation of transmission Raman scattering light. Light that irradiates an opaque material propagates in the material by repeated transmission and reflection. Consequently, we tested simulation of Raman scattering intensity using a simple model composed of several layers of thin materials to represent an opaque material. Raman scattering occurs each time the excitation light is repeatedly reflected and transmitted by the material molecules. As a result, first, we simulated the excitation light intensity at some depth in the material and calculated the Raman scattering intensity from the results; the intensity of the reflected Raman scattering appearing at the incident face and of the transmission Raman scattering appearing at the transmission face were simulated.

3.4.1 Excitation Light Simulation

As shown in Figure 8, the intensity of the excitation light at any depth in the test material can be considered as divided in two directions: in the transmission-face direction, and in the incident-face direction. Since the excitation light is repeatedly transmitted and reflected at each layer, the intensity of the excitation light at any depth can be found by summation using the transmittance T , reflectance R , and absorption α of each layer.

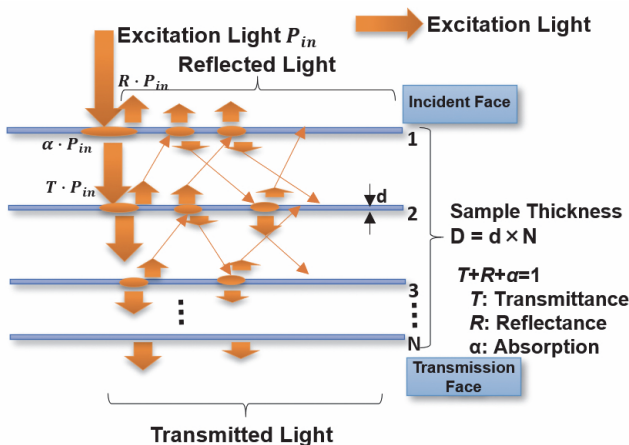


Figure 8 Excitation Light Power Calculation Model

We tested the simulation using layers of 0.13 mm thick paper. Figure 9 shows the actually measured excitation light transmittance and the simulated reflectance and transmittance. From transmittance of 8.4 dB at a paper thickness of 0.13 mm and the actually measured transmittance gradient of 5.4 dB/mm at paper thicknesses of more than 1 mm, transmittance of 86.3%, reflectance of 13.5% and absorption of 0.2% per

paper were obtained. And these values were applied to the simulation. The simulated transmittance is a close match with the actual measured value, suggesting this model can accurately calculate the intensity of the excitation light at any depth.

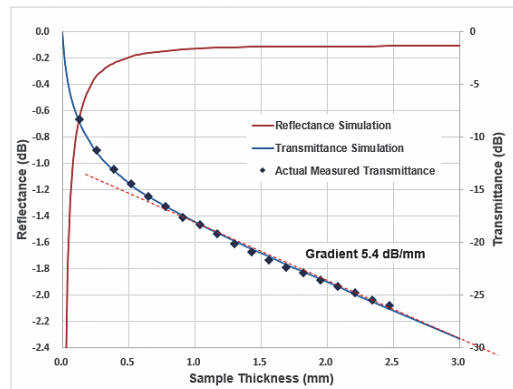


Figure 9 Excitation Light Reflectance and Transmittance

3.4.2 Raman Scattering Intensity Simulation

The next section explains how the intensity of the Raman scattering is found from the intensity of the excitation light in the test material as shown in Figure 10. If a layer is thin, the intensity of the Raman scattering is considered to be the same in both the transmission-face, and incident-face directions. Consequently, as with the excitation light, the total amount of the Raman scattering light repeatedly reflected and transmitted by each layer and appearing at the transmission and incident faces can be calculated.

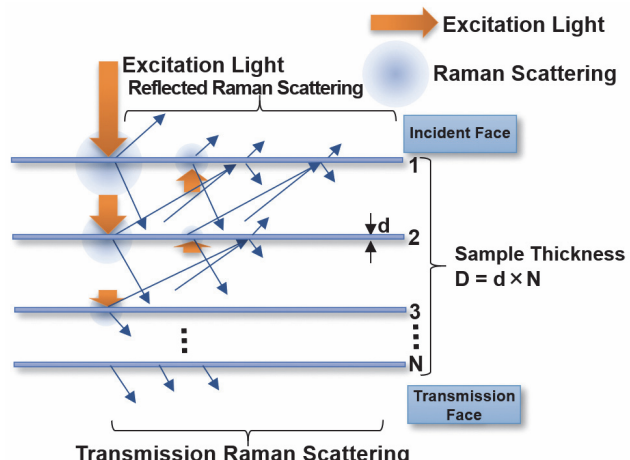


Figure 10 Raman Scattering Intensity Calculation Model

We measured the reflection Raman scattering intensity and transmission Raman scattering intensity by changing the thickness of the sample paper layers and compared with the simulations. The Raman spectrum for paper composed mainly of cellulose closely follows the pattern of crystalline cellulose used as an additive of pharmaceutical tablets to

adjust the concentration and maintain a constant tablet size (Figure 11). Since both paper and crystalline cellulose show fluorescence at an excitation-light wavelength of 785 nm, the data for the measured waveform in the figure was processed to eliminate the effect of fluorescence.

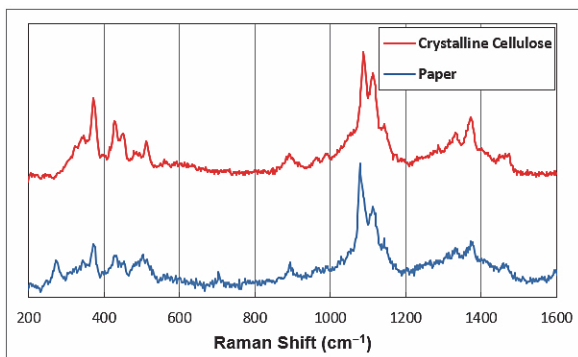


Figure 11 Raman Spectrum Paper and Crystalline Cellulose

Figure 12 shows the actual and simulated results for reflected Raman scattering intensity and transmission Raman scattering intensity. The optical intensity on the y-axis indicates the transmission Raman scattering intensity as 1 for a sample thickness of 0.1 mm. Both the simulated reflection Raman scattering intensity and transmission Raman scattering intensity closely match the actual measured values. From the figure, the reflection Raman scattering intensity increases as the test-material thickness increases and becomes constant when the paper thickness is 1.5 mm or more. Additionally, the transmission Raman scattering intensity increases up to a paper thickness of about 0.5 mm and then subsequently drops as thickness increases. When the test material is paper, the transmission Raman scattering intensity is maximum at a material thickness of 0.5 mm and is about 4 dB lower than the reflection Raman scattering intensity. Moreover, at a paper thickness of 2 mm, it is about 12 dB lower.

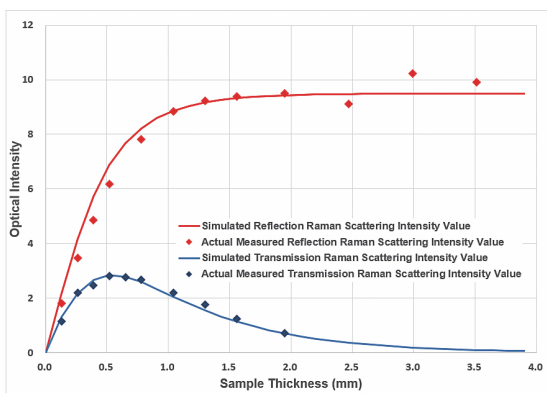


Figure 12 Reflected Raman Scattering Intensity and Transmission Raman Scattering Intensity

3.5 Transmission Raman Scattering Light Collection

Based on the above, collection of transmission Raman scattering suffers from two demerits compared to spot systems. First, since the Raman scattering is wide, to inject the Raman scattering light from all positions, the test material and fiber end faces must be separated and the incident angle must be small. Second, in comparison to reflection Raman scattering, the intensity of transmission Raman scattering is attenuated by material thickness.

For example, with a 2 mm thick material, when injecting transmission Raman scattering widened by a radius of 5 mm into an optical fiber with an NA of 0.22 and a core diameter of 200 μm , the intensity is about 46 dB lower than using the spot system. Currently, in comparison to spot analysis with commonly used microscope Raman equipment, using transmission Raman devices to measure Raman scattering in materials is difficult due to the extremely low Raman scattering intensity.

To collect the very small Raman scattering efficiently, the Raman scattering intensity can be increased by positioning a mirror close to the test material²⁾; other methods, such as using multiple optical fibers to collect the Raman scattering are being tested for commercial use. We will examine more efficient methods for coupling Raman scattering light to the fiber.

4 Quantifying from Raman Spectrum

We examined quantification (assay) of aqueous ethanol solutions using the Classical Least Squares (CLS) and Multiple Linear Regression (MLR) multivariate analysis methods for the Raman spectrum. In both methods, an unknown sample of the test material is assayed after calibration using a reference test material.

4.1 CLS

The CLS regression equation is expressed by Eq. (5)

$$A = KC + R_C \quad (5)$$

where, A is the spectrum matrix, C is the concentration matrix, K is the pure-ingredient spectrum matrix, and R_C is the residual. The spectrum matrix A plots the scattering strength versus wave number for an array of samples. The concentration matrix C lists the concentration ingredient ratio for each material. The purity ingredient spectrum matrix K plots the single spectrum of each ingredient in the mixture as an array of samples.

The assay procedure calculates K beforehand by calibration and then predicts concentration using the spectrum for the unknown concentration. To configure the calibration model, it is necessary to know the components and their densities; included errors, such as concentration errors and measurement errors, are reflected in the predicted concentration. When the pure-ingredient spectrum matrix found by calibration is K_c , the unknown concentration C_U is found from

$$C_U = \left((K_c^T K_c)^{-1} K_c^T \right) A_U \quad (6)$$

where, A_U is the unknown test-material spectrum matrix. The CLS method is independent of the strict peak wave number and since regression analysis is performed using measured spectrum values in a wide range of peaks, estimated values are less affected by measurement errors in comparison to the MLR method described next. However, if there are extensive unknown ingredients, the added spectra can have an adverse effect.

4.2 MLR

The general MLR regression method is expressed by Eq. (7)

$$C = FA + R_M \quad (7)$$

where, C is the concentration matrix, A is the spectrum matrix, F is the coefficient matrix, and R_M is the residual. This model predicts concentration directly and the coefficient F is found from the spectrum of a prepared test material of known concentration used for calibration. The calculation has the following two limitations. First, since the coefficient F cannot be calculated, the number of explanatory variables cannot exceed the number of test materials. In this example, the number of explanatory variables is the spectrum wave number and the test material is aqueous ethanol solutions of different densities. Second, the explanatory variable with Y multi-collinearity is not selected. Multi-collinearity includes multiple explanatory variables with high correlation having a high negative impact on the regression results. As shown, when the coefficient F_C is obtained from Eq. (7), the concentration C_U is found from the unknown spectrum A_U using Eq. (8).

$$C_U = F_C A_U = \left(C A^T (A A^T)^{-1} \right) A_U \quad (8)$$

Since MLR only uses minimum spectrum data for less than the number of samples due to the above-described restrictions, errors have a large impact. Moreover, if the selected data do not adequately capture the concentration data characteristics, the model has low usability.

4.3 Assaying Aqueous Ethanol Solutions

Figure 13 shows the Raman spectrums for six aqueous ethanol solutions of concentrations from 0.4% to 20%, and water (0%). From the pattern of spectrum peaks, it is clear that each amplitude changes in accordance with the concentration. The analysis data used the largest peak amplitude for both CLS and MLR. CLS used the wave number in the range of 850 to 900 cm^{-1} , while MLR used three data points near the peak of 870 cm^{-1} .

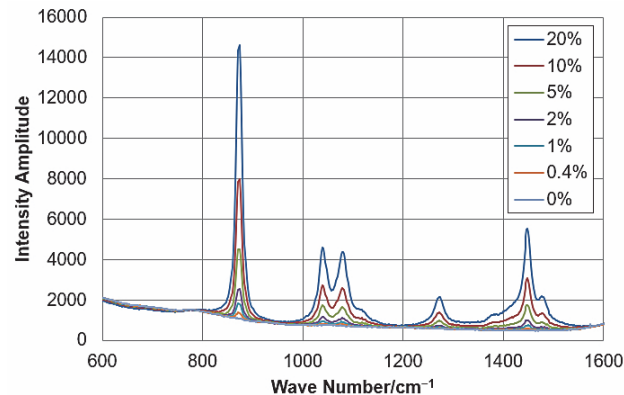


Figure 13 Raman Spectrum of Aqueous Ethanol Solutions

Figure 14 shows the concentration calibration results. There is no big difference between CLS and MLR, and the coefficient of determination R^2 of 0.9998 and 0.9992, respectively, are both very close to 1, showing that both predicted values are a good match for the actual values.

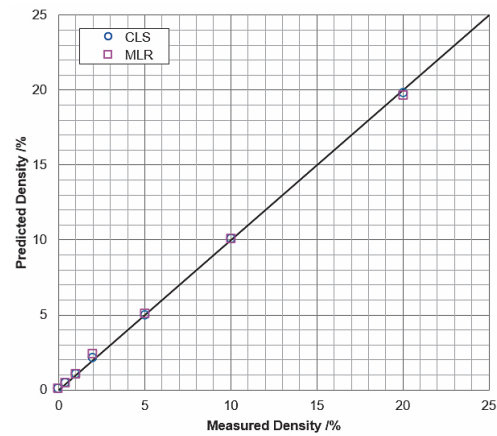


Figure 14 CLS and MLR Comparison using Aqueous Ethanol Concentration Calibration

To solve the problems of multicollinearity and unknown components depending on the spectrum data, we are examining Principal Component Regression (PCR), which combines principal component analysis with MLR, as well as Partial Least Squares (PLS) using the principal component considering the response variable.

5 Conclusions

This article explained our investigation into optical-fiber coupling efficiency and quantification of transmission Raman scattering intensity when collecting Raman scattering light to implement a high-sensitivity Raman spectrometer. Additionally, we introduced an analysis method using Raman spectrum analysis with an example of assaying aqueous ethanol solutions using basic CLS and MLR multivariate analyses.

Future research is targeted at investigating Raman spectrum analysis to achieve higher sensitivity by methods for improving the collection efficiency of Raman scattering and optimizing the overall spectrometer, light source, etc.

References

- 1) Hiro-o Hamaguchi, Koici Iwata (Eds.): "Raman Spectroscopy", Spectroscopy Series 1, The Spectroscopical Society of Japan (2015) (in Japanese)
- 2) Michael J. Pelletier, "Sensitivity-Enhanced Transmission Raman Spectroscopy", APPLIED SPECTROSCOPY Volume 67, Number 8 (2013)

Authors



Satoshi Makita
Technology Planning Department
Advanced Research Laboratory

Michihiko Ikeda
Technology Planning Department
Advanced Research Laboratory

Publicly available